Materials Science and Engineering C 49 (2015) 256–261

Contents lists available at ScienceDirect

Materials Science and Engineering C

journal homepage: www.elsevier.com/locate/msec

Arrayed three-dimensional structures designed to induce and maintain a cell pattern by a topographical effect on cell behavior

Takao Saito [a,*], Kay Teraoka [a], Kazuyoshi Ota [b]

[a] National Institute of Advanced Industrial Science and Technology (AIST), 2266-98 Anagahora, Shimoshidami, Moriyama-ku, Nagoya, Aichi 463-8560, Japan
[b] Otake Seisakusyo, Co., 103 Sukanaka, Hottsu-cho, Hashima, Gifu 501-6338, Japan

ARTICLE INFO

Article history:
Received 5 September 2014
Received in revised form 21 November 2014
Accepted 6 January 2015
Available online 8 January 2015

Keywords:
Surface topography
3-D structure
Groove
Cell behavior
Cellular microarray
Scaffold

ABSTRACT

We investigated the ability of the microscale topography of a three-dimensional (3-D) structure arrayed on the surface of a substrate to induce and maintain a cell pattern by controlling cell behavior. Arrayed 3-D structures having different topographical characteristics, i.e., geometry and dimension, were fabricated on the surface of glass substrates by masked sand blasting. Each 3-D structure was designed to have a unit composed of a planar island for cell growth and surrounding grooves exhibiting cell repellency. The principle of the cell repellency is based on the topographical control of cell attachment, spreading, growth, and differentiation by utilizing the spatially restricted microenvironment of the grooves. Grooves with a width of less than approximately 116 μm and a depth of approximately 108 μm formed narrow V-shapes with a dihedral angle of less than approximately 44.4°. Cell culture experiments using osteoblast-like cells demonstrated that these narrow V-shaped grooves had sufficient cell repellency to form and maintain a cell pattern on the surface for at least 14 days. From the present study, arrayed 3-D structures designed to have narrow V-shaped grooves with optimal topographical characteristics for cell repellency are promising for the formation of stable cell patterns for creating novel cell microarray platforms without using conventional protein/cell-repellent chemicals.

1. Introduction

Many biomedical devices such as microarrays, drug delivery systems, biosensors, and scaffolds for tissue engineering have been recently developed for the study and manipulation of biomolecules, and they have proven to be valuable experimental tools for solving many biologically based problems [1]. Microarray technology in particular has become a crucial tool for large-scale and high-throughput biological experiments, as it enables fast, easy, and parallel detection of thousands of addressable elements in a single experiment under identical conditions [2]. Such microarrays of DNA, proteins, and cells are now becoming important tools for exploring genomics, proteomics, and cellomics.

Cellular microarrays have recently received considerable attention because of their important roles in fundamental cell biology, cell-based biosensors, and biological microelectromechanical systems [3]. They are being developed for various cellular analyses of the effects of gene expression, cellular reactions to the biomolecular environment, and cell surface molecule profiles [4,5]. Cellular microarrays offer an additional advantage in their ability to analyze the expression of genes and the function of proteins in a living cell where all of the cellular machinery is present to ensure correct function, thereby facilitating the high-throughput validation of tens of thousands of gene and protein targets [6].

One effective method for creating cellular microarray platforms is based on the patterning of protein/cell-repellant chemicals, such as hydrophilic polyethylene glycol (PEG) derivatives [7], layered on microarray surfaces. These chemicals reduce the non-specific adsorption of cell-adhesive proteins such as collagen, fibronectin, and vitronectin from culture media, and cell patterning is consequently formed on patterned surfaces composed of cell-repellant and cell-adhesive regions. However, the problem with using conventional protein/cell-repellant chemicals is that the formed cell patterns are temporary and break easily within several days because of increased desorption from the surfaces and gradual adsorption of cell-adhesive proteins. Rather than using hydrophilic chemicals such as PEG derivatives, we previously examined block cell adhesion utilizing superhydrophobicity generated by the lotus effect of a perfluoroalkyl isocyanate layer on an oxidized aluminum surface with nanosize topographical features [8,9]. Although a complete cell pattern was formed on the micropatterned perfluoroalkyl isocyanate layer one day after seeding, the formed cell pattern broke after a few days of culture, indicating that the superhydrophobic coating was also not effective for long-term cell repellency.

To investigate cellular responses to physically structured surfaces, the effects of sub-micrometer- and micrometer-scaled surface roughness were previously examined along with the sequential events of cell adhesion, growth, differentiation, and mineralization [10]. The

* Corresponding author.
E-mail address: t-saito@aist.go.jp (T. Saito).

http://dx.doi.org/10.1016/j.msec.2015.01.021
0928-4931/

results suggested that the reduction of cell growth on rough-surfaced substrates was closely related to rounding of cell bodies caused by surface topography at the micrometer scale, accompanied by the disassembly of actin filaments.

Considering the suppression of cell growth on rough-surfaced substrates, in the present study we examined a different strategy to develop cell repellency using tailored 3-D structures rather than chemicals to induce and maintain cell patterns for creating novel cellular microarrays. The 3-D structure consisted of a planar island adequate for cell growth and surrounding grooves for cell repellency induced by surface topography, thus affecting cell shape and spreading through a cell-surface phenomenon called contact guidance [11,12]. The cell repellency of a groove is directly influenced by its geometry and dimension, i.e., its cross-section shape, width, and depth, in addition to surface roughness. Topographical control of cellular responses is a purely physical and biologically non-invasive method without chemicals; therefore, it would be stable against non-specific adsorption of adhesive proteins and effective for long-term cell repellency [13,14]. In the present study, to develop novel cell microarray platforms that maintain cell patterns for a longer duration, we focused on the topographical design of a 3-D structure and examined the effects of topographical characteristics of the grooves, such as geometry and dimension, on cell attachment, growth, differentiation, and pattern formation.

2. Materials and methods

2.1. Substrate preparation

To prepare substrates with arrayed 3-D structures, masked sand blasting was employed to etch the surface of slide glasses (#S1112; Matsunami Glass; Kishiwada, Japan) by using a sand blaster (ELP-4TR; Elfo-tec; Nagoya; Japan). Four types of mask patterns were prepared on photosensitive dry films to generate different 3-D structures. Each mask pattern (A-D) was composed of a square-shaped planar island ($250 \times 250\ \mu m^2$) and surrounding grooves with a width of 50, 100, 150, and 300 μm, respectively. The grooves were etched to have the same depth of 100 μm by sand blasting with a #1200 mesh abrasive with a particle size of approximately 9.5 ± 0.8 μm. Before the cell culture experiments, the surfaces of the etched substrates were thoroughly cleaned by sonication in acetone and then sterilized in 70% ethanol for 10 min.

2.2. Morphological characterization of 3-D structures

Bird's-eye view images of the arrayed 3-D structures fabricated on the surfaces of the slide glasses were taken at a dip of approximately 45°, using a laser microscope (VK-X200; Keyence; Tokyo, Japan). The cross-sectional shapes of the grooves were determined by X-ray micro-computed tomography (μCT; SMX-160LT; Shimadzu; Kyoto; Japan), using a LaB_6 filament and a minimum focus dimension of 0.4 μm. The dimensions of each groove including width, depth, dihedral angle, and radius of curvature at the bottom were measured using images obtained by laser microscopy and μCT.

2.3. Cell culture

The murine osteoblast-like cell line MC3T3-E1 was purchased from Riken Cell Bank (Tsukuba, Japan). The cells were maintained and grown in Minimum Essential Medium-α (α-MEM, Life Technologies, CA) containing 10% fetal bovine serum and antibiotics in a humidified 5% CO_2 balanced-air incubator at 37 °C [10]. The differentiation medium was prepared by adding 50 μg/ml ascorbic acid and 10 mM β-glycerophosphate to the growth medium. Cells with an average diameter of 19.6 ± 1.4 μm and average circularity of 0.84 ± 0.06 were plated onto the sterilized substrates at approximately $3–5 \times 10^4$ cells/cm^2 in 12-well plates and then cultured in growth medium for 1 week and in differentiation medium for the next week. Cell culture experiments of the same conditions were duplicated to investigate cellular responses to the arrayed 3-D structures.

2.4. Observation of cell behavior

2.4.1. Fluorescence microscopy

The cells cultured on the substrates were fixed in 3.7% formaldehyde in phosphate-buffered saline (PBS) for 10 min and permeabilized using 0.1% Triton X-100 in PBS for 5 min at room temperature. Actin filaments were stained with 5 U/mL rhodamine phalloidin in PBS containing 1% bovine serum albumin (BSA) for 20 min. The nuclei were stained with 0.3 μM 4′, 6-diamidino-2-phenylindole, dihydrochloride (DAPI), a DNA binding dye, in PBS for 5 min at room temperature. Fluorescence images of actin filaments and nuclei were obtained using a fluorescence microscope (FM; BX51; Olympus; Tokyo; Japan) equipped with a WUS filter set (excitation filter: 330–385 nm; emission filter: 420 nm) and a WG filter set (excitation filter: 510–550 nm; emission filter: 590 nm), respectively. If necessary, images were electronically combined to generate a co-localized image. Two or more FM images were taken with a different view for each specimen.

2.4.2. Field emission scanning electron microscopy

The cells cultured on the substrates were fixed in 2.5% glutaraldehyde for 2 h at 4 °C, immobilized in 1.0% osmium for 2 h at 4 °C, dehydrated through a series of increasing concentrations (50%, 70%, 80%, 90%, and 100%) of ethanol in water for 30 min, and finally dried with *tert*-butyl alcohol in a freeze dryer. The dried samples were coated with sputtered Pt–Pd. Two or more images with a different view were taken via field emission scanning electron microscopy (FESEM; S-4300; Hitachi High-Technologies; Tokyo; Japan).

2.4.3. Bright field microscopy

Differentiated cells with alkaline phosphatase (ALP) activity were histochemically detected using an ALP kit (86R; Sigma-Aldrich; St. Louis; MO). In brief, the cells on the substrates were fixed with citrate–acetone–formaldehyde solution for 30 s and rinsed with Milli-Q water. Then, the cells were incubated in an alkaline dye mixture for 15 min, rinsed with Milli-Q water, and counterstained with hematoxylin solution for 2 min. After thorough rinsing with Milli-Q water and drying, ALP-positive cells were observed via bright-field microscopy (BX51) and two or more images were taken with a different view.

3. Results and discussion

3.1. Fabrication and characterization of the 3-D structures

From previous results on the effects of surface roughness on the cell adhesion, growth, and differentiation of MC3T3-E1 cells [10], we assumed that cell growth and function could be controlled by structured surfaces at the micrometer scale. Based on this assumption regarding cell-surface interactions, in the present study we focused on how the geometry and dimensions of 3-D structured surfaces affect cell behavior. We designed and fabricated arrayed 3-D structures composed of a planar island and surrounding grooves at the micrometer scale on the surface of a glass substrate, and then examined the effect of the geometry and dimensions of the grooves on cell behavior, i.e., cell attachment, spreading, growth, differentiation, and pattern formation.

Four types of mask patterns were prepared and slide glasses were sand-blasted through these masks. A #1200 mesh abrasive was used to etch different arrayed 3-D structures on the glass surfaces at a depth of approximately 100 μm. Bird's-eye views of the arrayed 3-D structures on slide glasses fabricated by masked sand blasting were obtained via laser microscopy [Fig. 1(A)–(D)]. The surface roughness of the sand-blasted surface was measured to be 0.50 ± 0.05 μm. Cross-section images of the grooves obtained via μCT are shown in the insets of

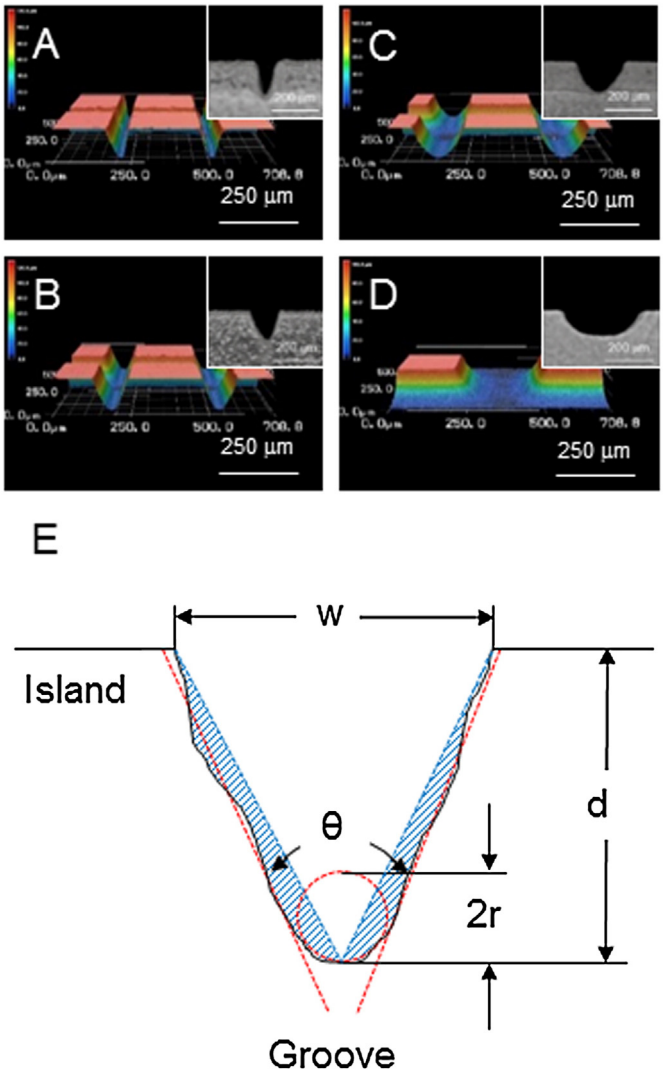

Fig. 1. (A–D) Laser microscopic images of the arrayed 3-D structures fabricated by masked sand blasting and CT internal images of the grooves (insets). (E) Schematic drawing of the cross-section of a V-shaped groove. w: width of the groove; d: depth of the groove; θ: dihedral angle of the groove; r: radius of the curvature at the groove bottom; hatch: abraded area from a V-shaped groove.

Fig. 1(A)–(D). The dimensions of the grooves schematically drawn in Fig. 1(E) were measured by laser microscopy, and the results are summarized in Table 1. The width and depth of each groove etched on slide glasses were larger than the typical length scale of a MC3T3-E1 cell, for which the average diameter was estimated to be 19.6 ± 1.4 µm. Grooves A and B had V-shaped cross-sections, whereas grooves C and D had U-shaped cross-sections, as confirmed by cross-section µCT images [Fig. 1(A)–(D)] and the calculated abrasion ratio, defined as the value of the deviation from a V-shaped groove (Table 1). As the width of the groove increased, the deviation and the radius of the curvature in the bottom of the groove increased, resulting in a U-shaped groove rather than a V-shaped groove. Masked sand blasting with a #1200 mesh abrasive made the cross section of the grooves V-shaped or U-shaped, depending on the width of the groove.

3.2. Cell behavior on the 3-D structures

3.2.1. Cell attachment

The nuclei of MC3T3-E1 cells adherent to the 3-D structured substrates one day after plating were stained with DAPI to visualize the localization of the cells on the surfaces. Although the number of cells that adhered to the square-shaped planar islands of the 3-D structures was unrelated to the width of the groove (left panels in Fig. 2), fewer cells adhered to the V-shaped grooves A and B (right panels in Fig. 2). A similar effect, called guided cell adhesion, was reported for fibroblasts cultured on edged surfaces [15] and keratinocyte stem cells cultured on micropatterned poly(lactide-co-glycolide)/polyurethane substrates [16]. However, little is known regarding the mechanisms underlying this phenomenon. It is also not clear why fewer cells adhered to these V-shaped grooves in the present study. Further investigations concerning the inhibitory effect of the V-shaped groove on initial cell attachment are currently underway.

Thus, different adhesion patterns of the cells were achieved during seeding. This cell repellency of the V-shaped grooves that prevented initial cell attachment is favorable for later cell pattern formation in the arrayed 3-D structures. In addition to this topographical repulsion of initial cell attachment, cell pattern formation and stability require subsequent suppression of cell growth and migration on the V-shaped grooves.

3.2.2. Cell morphology

The quality of the first phase of cell/material interactions induced by surface characteristics of materials, such as topography, chemistry, or surface energy, influences cell morphology, capacity for cell growth, and differentiation [17]. The topography at the nanometer scale affects sub-cellular behavior such as the organization of cell adhesion molecule receptors, whereas at the micrometer level, cellular and supra-cellular characteristics such as cell morphology and migration are influenced [10,12,18]. For instance, a previous study by Chen et al. [19] demonstrated using capillary endothelial cells that cell shape is the critical determinant that governs whether individual cells grow or die. Miura and Fujimoto [20] reported that cells attached on a closely packed particle monolayer had a stretched narrow stalk-like shape and that cell growth was suppressed relative to a flat surface, and concluded that cell extension and shape could be related to cell growth. Based on these previous findings, we assumed that direct geometric control of cell shape and growth by designed 3-D structures at the micrometer level can be applicable for cell pattern formation.

The morphology of the attached MC3T3-E1 cells one day after plating on the substrates was observed via FESEM. Representative images are shown in the left panels of Fig. 3 to illustrate the dependence of cell morphology on surface topography. While the cells on a planar island exhibited more spreading and a more flattened morphology, those on grooves A and B had an irregular morphology resulting from anisotropic stresses generated by the geometry and dimension of the

Table 1
The dimensions of the grooves fabricated by masked sand blasting on a glass substrate evaluated via laser microscopy and µCT; a schematic representation is shown in Fig. 1(E). Results reported as means ± standard deviation; n = 5.

Sample	w: width (µm)	d: depth (µm)	Abrasion ratio ()	Shape	θ: dihedral angle (°)	r: radius of curvature (µm)
A	69.3 ± 3.0	92.9 ± 2.0	10.9 ± 4.4	V-shaped	24.7 ± 0.3	8.5 ± 1.6
B	115.9 ± 2.9	107.5 ± 1.7	19.2 ± 2.4	V-shaped	44.4 ± 0.6	16.2 ± 3.7
C	164.3 ± 2.6	101.7 ± 0.6	31.1 ± 1.8	U-shaped		51.3 ± 5.6
D	314.0 ± 1.2	97.1 ± 1.0	46.9 ± 1.8	U-shaped		206.1 ± 2.7

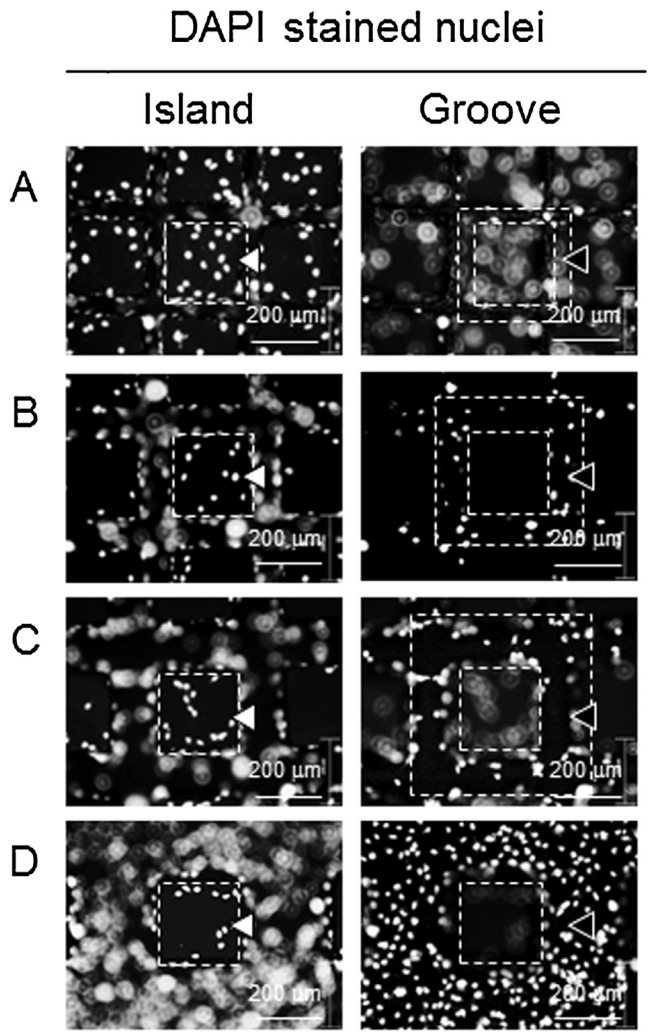

Fig. 2. FM images of DAPI-stained nuclei of MC3T3-E1 cells attached to the substrates (A–D) one day after plating. Fluorescence images were obtained by staining the nuclei of the cells attached to a square-shaped planar island (left panels, white arrow head) and surrounding grooves (right panels, black arrow head) with DAPI.

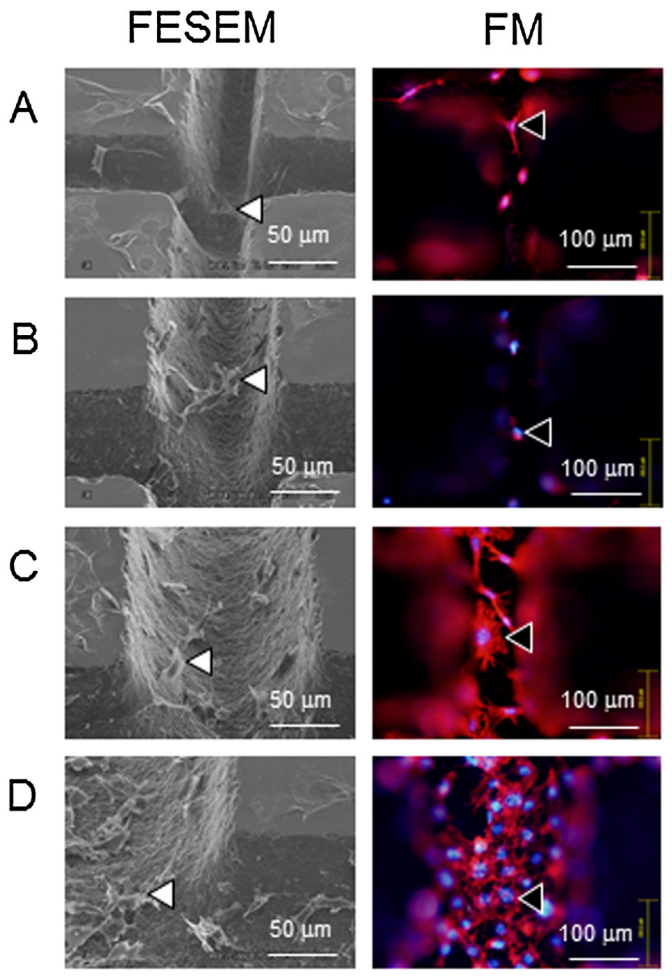

Fig. 3. FESEM (left panel) and FM (right panel) images of MC3T3-E1 cells attached to the grooves of the substrates (A–D) one day after plating. Fluorescence images were obtained by double-staining of the cells with rhodamine phalloidin and DAPI for actin filament and nuclear staining, respectively. White arrowhead: cell attached to the surface; black arrowhead: double-stained cell.

narrow V-shaped grooves. These results clearly indicate that cell morphology is significantly influenced by the surface geometry of the substrates where cells attach.

3.2.3. Actin filament organization

The shapes of the cells reacting to the surrounding topography may subject the cytoskeleton to strain [18]. The actin cytoskeleton has the unique capability of integrating signaling and structural elements to regulate cell function [21]. We observed actin filament organization in stress fibers on the 3-D structures one day after plating via FM. As shown in the right panel in Fig. 3, the actin cytoskeleton was diffuse with less stress fiber formation, especially in cells attached to V-shaped grooves A and B. Therefore, the irregular cell morphology with lower stress fiber formation observed on the V-shaped grooves A and B in this study may also be explained by the geometric restriction of cell spreading caused by the narrowness of the grooves and their V-shaped cross-section. Considering that actin stress fibers play an important role in many cellular functions [22], the poor organization of stress fibers observed in the cells attached to V-shaped grooves suggests a negative effect on the later development of cellular characteristics such as growth, migration and differentiation.

3.3. Cell pattern formation on the arrayed 3-D structures

3.3.1. DAPI staining

The nuclei of cells cultured on the substrates for 14 days were stained with DAPI to determine whether the cell patterns were formed and maintained on the arrayed 3-D structures. When live, healthy cells are exposed to DAPI, staining is restricted to the chromatin. Staining in the cytoplasm suggests a lack of integrity of the cellular membrane and is a sign of necrosis [23]. As shown in the left panels in Fig. 4, 'healthy' nuclei, which were round or oval with a distinct nuclear outline and uniform DAPI staining, were present on a square-shaped planar island of each type of 3-D structure. However, few healthy nuclei were observed on grooves A and B, as shown in the right panels in Fig. 4. Furthermore, the nuclei of these cells were unstructured, suggesting that these cells lost their intrinsic cell functions or were dead. These results indicate that the cell patterns were formed and maintained up to day 14 on the arrayed 3-D structures having narrow V-shaped grooves.

3.3.2. ALP positive staining

Changing the growth medium to the differentiation medium at day 7 after plating induced the MC3T3-E1 cells on the substrates to differentiate and express osteoblastic markers such as ALP, osteocalcin, and parathyroid hormone receptor [24]. ALP activity is an established marker for the osteoblast phenotype [10,25], and its increase reflects a shift to

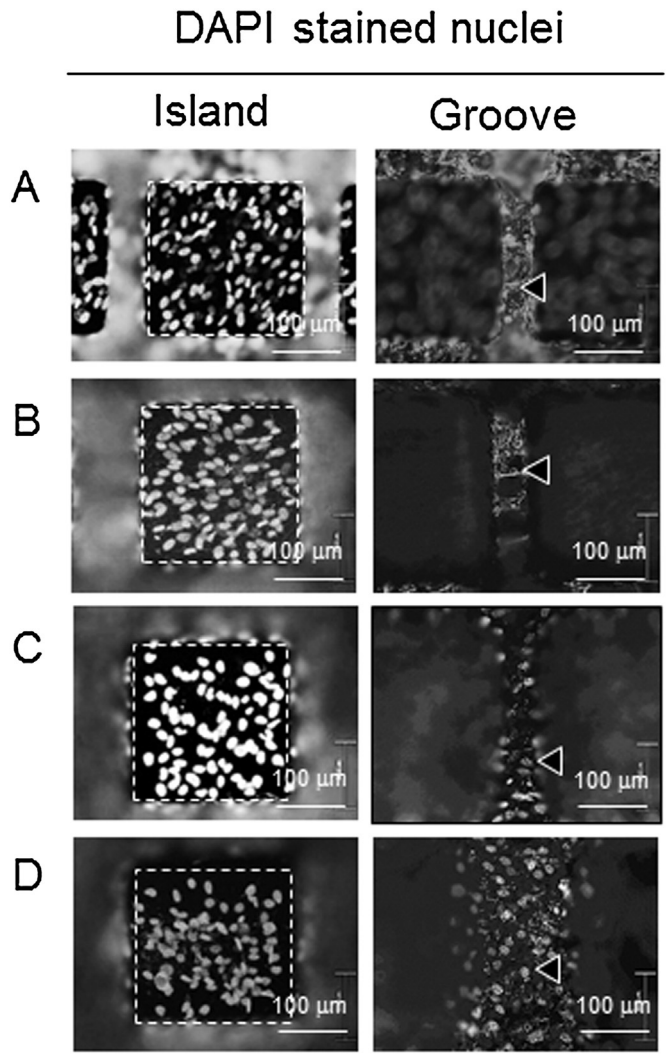

Fig. 4. FM images of DAPI-stained nuclei of MC3T3-E1 cells attached to the substrates (A–D) at day 14 after plating. Black arrowhead: DAPI-stained nuclei.

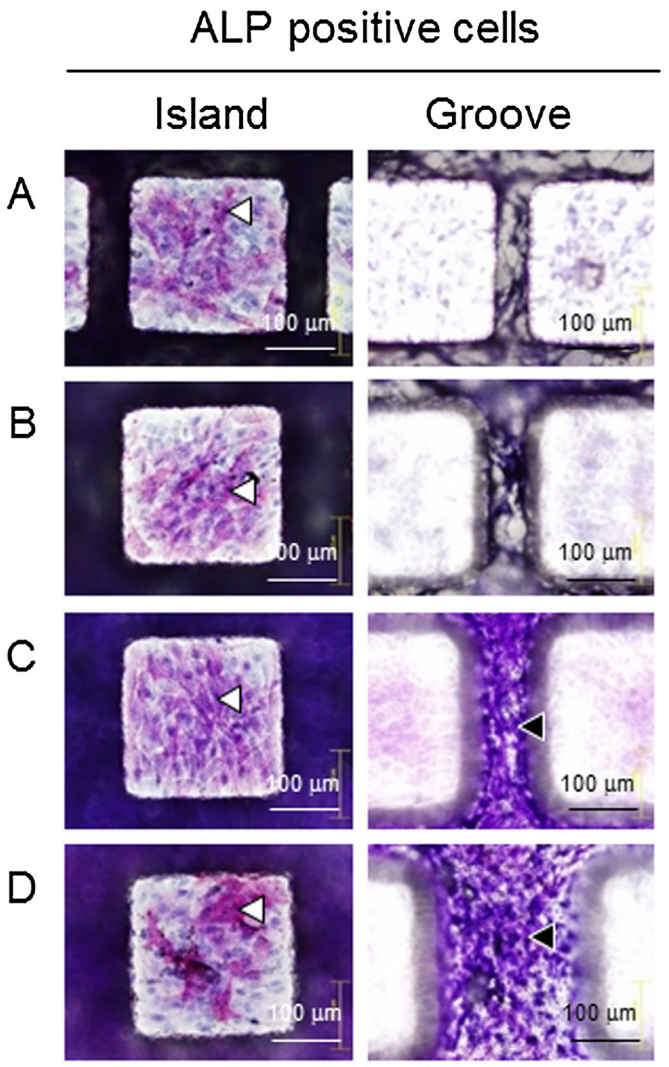

Fig. 5. ALP-positive cells on the structures (A–D) at day 14 after plating. ALP-positive cell: pink (white arrowhead); ALP-negative cell: bluish-purple (black arrowhead). (For interpretation of the references to color in this figure legend, the reader is referred to the web version of this article.)

a more differentiated state [26,27]. The location of the differentiated cells on the 3-D structures at day 14 was determined by histochemical staining of ALP-positive cells. As shown in Fig. 5, the cells on the square-shaped planar island of each type of 3-D structure were differentiated, but none of the cells on the groove were differentiated. Counterstaining with hematoxylin indicated that the cell population in the grooves increased as the width of the grooves increased. In grooves A and B, few cells were present, which is consistent with the results of DAPI staining shown in Fig. 4.

3.3.3. Cell pattern formation

The role of microscale topography in regulating cell adhesion and morphology has been extensively studied and such topography has great potential for application as biomaterials. Nikkhah et al. [12] summarized various microscale topographies with dimensions greater than 1 μm and isotropic features, including grooves, pillars, wells, and pits. It should be noted that cellular responses to microscale topographies depend on each cell type. Hamilton et al. [15] demonstrated that osteoblasts and epithelial cells respond differently to the same topographies of precisely defined tapered pits produced by microfabrication, and they suggested that the cellular responses to surface topography are strongly influenced by the inherent functional properties of each cell.

The present study demonstrates that MC3T3-E1 cells can normally grow and differentiate on a square-shaped planar island but not on narrow V-shaped grooves in the 3-D structures, suggesting that cell patterns can be formed and maintained in arrayed 3-D structures containing planar islands for cell growth and grooves with optimal topographical characteristics for cell repellency. Thus, the topographical control of cell growth and migration investigated here is potentially applicable to fabricating novel cell microarray platforms. We believe that the present study represents the starting point of another application of substrate topography with anisotropic V-shaped grooves, i.e., to create a novel cellular microarray platforms. Although the crucial parameters determining the cell-surface reaction are largely unknown, we have determined that the topographical characteristics of surface structures, such as the geometry and dimensions of V-shaped grooves, play an important role in determining cell fate by controlling cell behavior. Further studies on creating novel cellular microarray platforms are now underway, including cell-repelling experiments with the derivative 3-D structures shown in Fig. 6, one with multiple lanes, and the other with converted multiple lanes and a well structure derived from a V-shaped groove surrounded with a single lane.

4. Conclusions

Here, we present a concept to create novel cellular microarray platforms using topographically designed structures exhibiting long-term

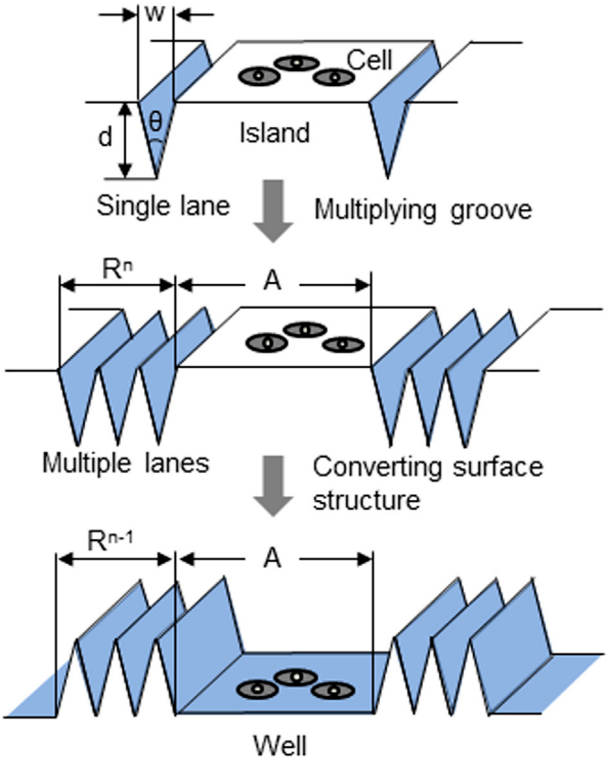

Fig. 6. Schematic drawings of arrayed 3-D structure derivatives, one with multiple lanes (middle panel) and the other with converted multiple lanes (lower panel), derived from a V-shaped groove surrounded with a single lane (upper panel) investigated in this study. R, R^{n-1}, R^n: cell-repellent region; A: cell-adhesive region.

cell repellency rather than conventional cell-repellent chemicals. Arrays of 3-D structures composed of a planar island and surrounding grooves were fabricated on the surfaces of glass substrates by masked sand blasting. We investigated the geometry and dimensions of the 3-D structures optimal for inducing and maintaining cell patterns by topographical control of cell behavior, i.e., cell attachment, spreading, growth, and differentiation. The present results indicate that grooves with a narrow V-shaped cross-section showed sufficient cell repellency to form and maintain cell patterns on the surface for 14 days. Considering that the osteoblast-like cells that adhered to the planar islands grew normally and differentiated to an osteoblastic phenotype, arrayed 3-D structures designed to have planar islands for cell growth and grooves having the optimal topographical characteristics for cell repellency are promising platforms for the creation of stable cell microarrays applicable to fundamental and applied biology studies in the near future. Furthermore, the development of cell-repellent surfaces with 3-D structures is promising for generating not only cellular microarray platforms but also various next-generation scaffolds and biomedical devices that contact cells in vitro and in vivo because of their lack of toxicity and lack of chemical contamination.

Acknowledgment

We would like to thank K. Ochi (Keyence Co., Osaka, Japan) for technical support in observing the geometries of the grooves and determining their dimensions by laser microscopy.

References

[1] A.L. Hook, H. Thissen, N.H. Voelcker, Trends Biotechnol. 24 (2006) 471.
[2] Y. Ito, M. Nogawaa, M. Takedab, T. Shibuyab, Biomaterials 26 (2005) 211.
[3] M. Veiseh, B.T. Wickes, D.G. Castner, M. Zhang, Biomaterials 25 (2004) 3315.
[4] B. Angres, Expert. Rev. Mol. Diagn. 5 (2005) 769.
[5] T.G. Fernandes, M.M. Diogo, D.S. Clark, J.S. Dordick, J.M.S. Cabral1, Trends Biotechnol. 27 (2009) 342.
[6] S. Mousses, A. Kallioniemi, P. Kauraniemi, A. Elkahloun, O.-P. Kallioniemi, Curr. Opin. Chem. Biol. 6 (2002) 97.
[7] K.L. Prime, G.M. Whitesides, J. Am. Chem. Soc. 115 (1993) 10714.
[8] A. Hozumi, B. Kim, T.J. McCarthy, Langmuir 25 (2009) 6834.
[9] T. Saito, H. Goto, M. Yagihashi, A. Hozumi, Chem. Lett. 39 (2010) 1048.
[10] T. Saito, H. Hayashi, T. Kameyama, M. Hishida, K. Nagai, K. Teraoka, K. Kato, Mater. Sci. Eng. C 30 (2010) 1.
[11] P. Rørth, Dev. Cell 20 (2011) 9.
[12] M. Nikkhah, F. Edalat, S. Manoucheri, A. Khademhosseini, Biomaterials 33 (2012) 5230.
[13] J.Y. Lim, H.J. Donahue, Tissue Eng. 13 (2007) 1879.
[14] D.H. Kim, K. Han, K. Gupta, K.W. Kwon, K.Y. Suh, A. Levchenko, Biomaterials 30 (2009) 5433.
[15] D.W. Hamilton, B. Chehroudi, D.M. Brunette, Biomaterials 28 (2007) 2281.
[16] I.A. Paun, M. Mihailescu, B. Calenic, C.R. Luculescu, M. Greabu, M. Dinescu, Appl. Surf. Sci. 278 (2013) 166.
[17] K. Anselme, Biomaterials 21 (2000) 667.
[18] L. Ponsonnet, V. Comte, A. Othmane, C. Lagneau, M. Charbonnier, M. Lissac, N. Jaffrezic, Mater. Sci. Eng. C 21 (2002) 157.
[19] C.S. Chen, M. Mrksich, S. Huang, G.M. Whitesides, D.E. Ingber, Science 276 (1997) 1425.
[20] M. Miura, K. Fujimoto, Colloid Surf. B 53 (2006) 245.
[21] G.F. Weber, A.S. Menko, Dev. Biol. 295 (2006) 714.
[22] R.D. Mullins, S.D. Hansen, Curr. Opin. Cell Biol. 25 (2013) 6.
[23] A. Jurisicova, S. Varmuza, R.F. Casper, Mol. Hum. Reprod. 2 (1996) 93.
[24] N.F.- Zelman, H. Hörandner, E. Luegmayr, F. Varga, A. Ellinger, M.P.M. Erlee, K. Klaushofer, Bone 20 (1997) 225.
[25] A. Ehara, K. Ogata, S. Imazato, S. Ebisu, T. Nakano, Y. Umakoshi, Biomaterials 24 (2003) 831.
[26] J.E. Aubin, F. Liu, L. Malaval, A.K. Gupta, Bone 17 (1995) 77S.
[27] L. Malaval, F. Liu, P. Roche, J.E. Aubin, J. Cell. Biochem. 74 (1999) 616.